Supplement of Atmos. Chem. Phys., 26, 10029–10042, 2026
https://doi.org/10.5194/acp-26-10029-2026-supplement

Atmospheric Chemistry and Physics
Open Access

Supplement of

High yields of formic acid and acetic acid during multi-generational oxidation of toluene

Hengqing Shen et al.

Correspondence to: Liubin Huang (hliubin@sdu.edu.cn) and Zhongming Chen (zmchen@pku.edu.cn)

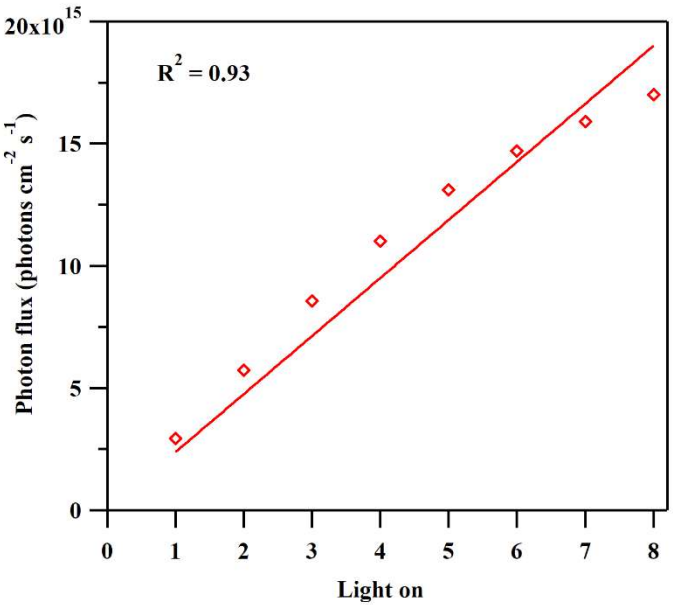

Figure S1. Photon fluxes estimated by the model with different lamps illuminated (up to 8).

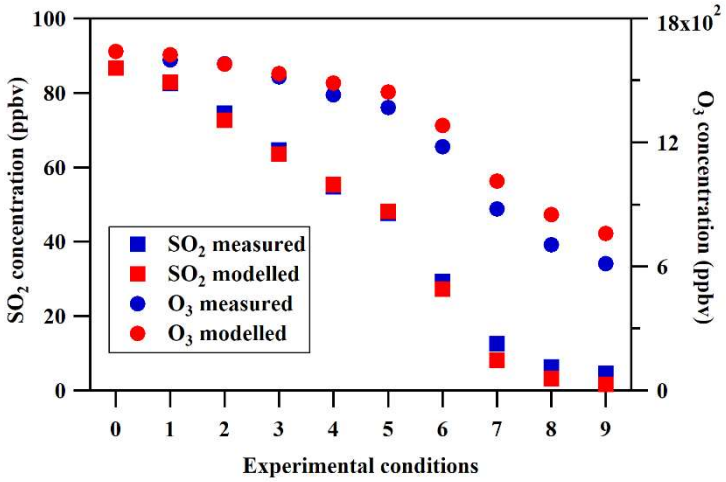

Figure S2. Comparison of the decay of SO_2 and O_3 measured in the OFR and simulated by the model. The experimental conditions of 0–9 correspond to no lamp illuminated (#0), one lamp illuminated with the residence times of 3.9 s (#1), 15.8 s (#2), 27.5 s (#3), 39.3 s (#4), and 51.0 s (#5), and to 2 (#6), 4 (#7), 6 (#8), and 8 (#9) lamps illuminated with the residence time of 51.0 s.

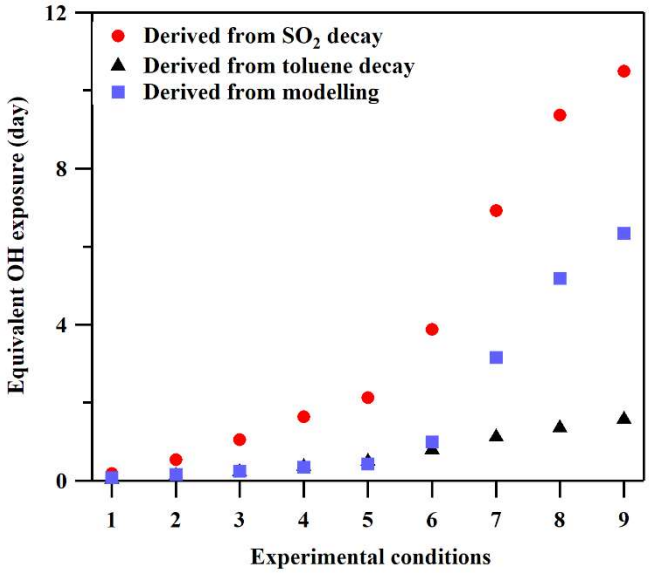

Figure S3. •OH exposures derived from three different methods (SO_2 decay, toluene decay, and modeling). The experimental conditions of 1–9 correspond to one lamp illuminated with the residence time of 3.9 s (#1), 15.8 s (#2), 27.5 s (#3), 39.3 s (#4), and 51.0 s (#5), and to 2 (#6), 4 (#7), 6 (#8), and 8 (#9) lamps illuminated with the residence time of 51.0 s.

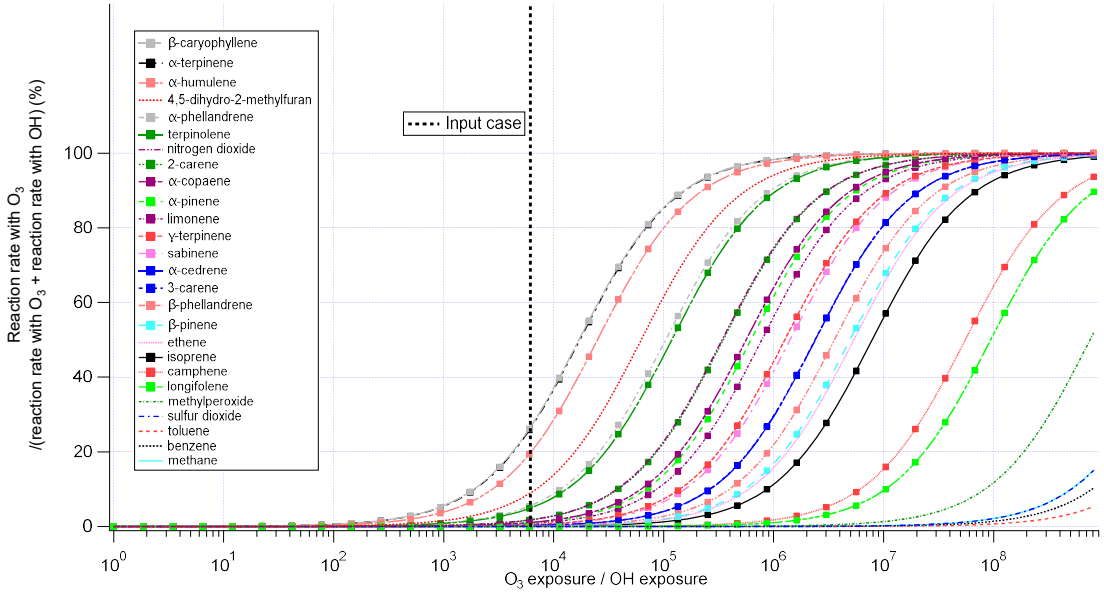

Figure S4. Relative contributions of O_3 reactions versus •OH reactions in the oxidation flow reactor under the experimental conditions used in this study: a 254 nm photon flux of ~3.0 × 10^{15} photons cm^{-2} s^{-1}, an initial O_3 concentration of 1.58 ppmv, and a relative humidity of 70%. For each species, the contribution of an O_3 reaction was estimated from the pseudo-first-order rate coefficient $k_{O3}[O_3]$, whereas the contribution of •OH oxidation was estimated from k_{OH}[•OH].

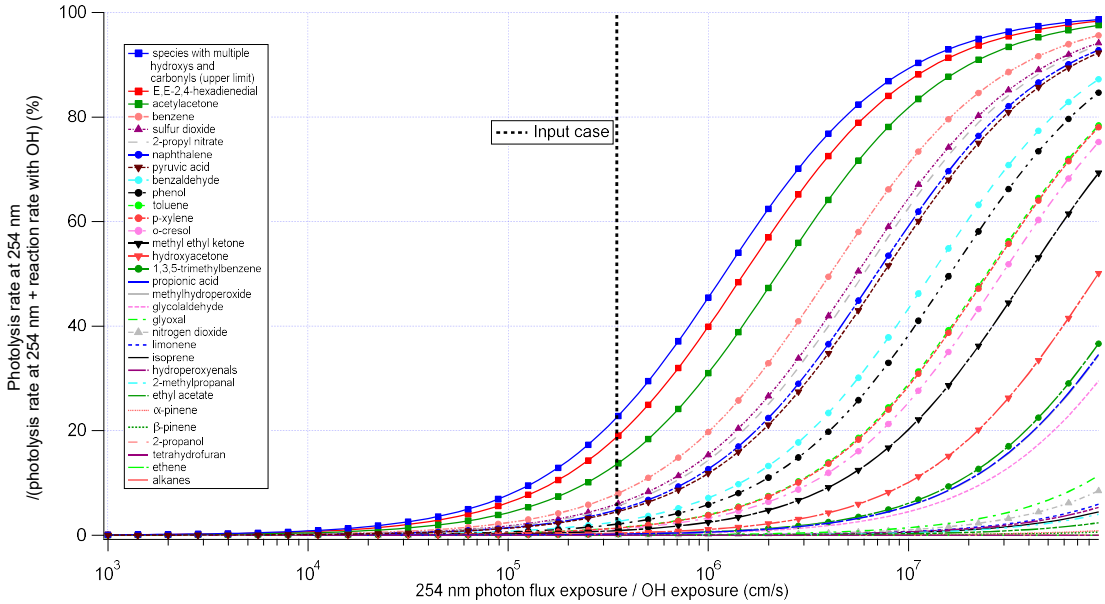

Figure S5. Relative contributions of 254 nm photolysis versus •OH reactions in the oxidation flow reactor under the experimental conditions used in this study: a 254 nm photon flux of ~3.0 × 10^{15} photons cm^{-2} s^{-1}, an initial O_3 concentration of 1.58 ppmv, and a relative humidity of 70%. The contribution of direct 254 nm photolysis was estimated from the corresponding photolysis frequency and compared with k_{OH}[•OH].

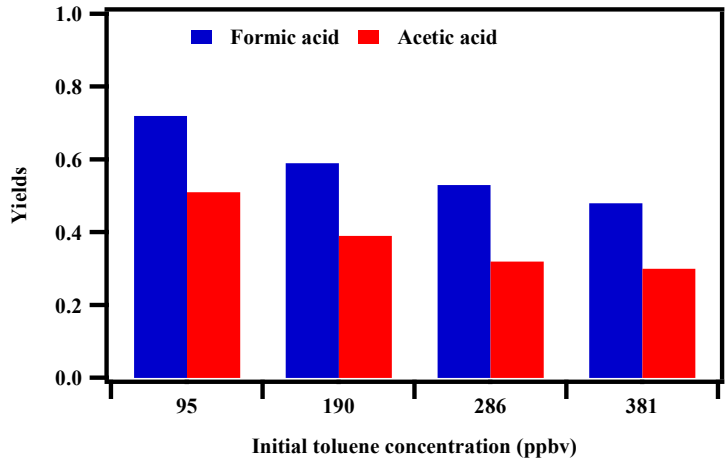

Figure S6. Effects of initial toluene concentrations on the yields of formic acid and acetic acid.

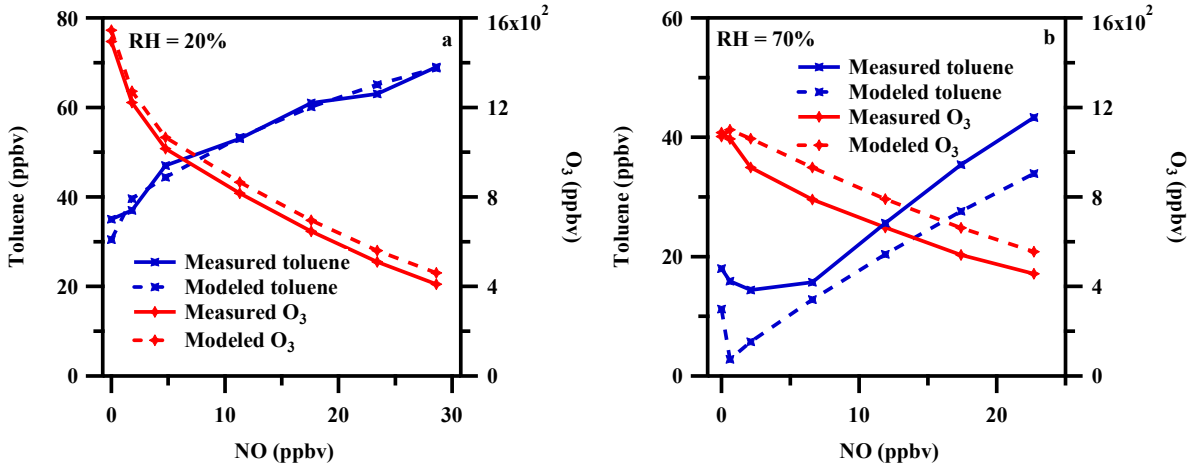

Figure S7. Comparison of observed and simulated toluene and O_3 concentrations as a function of NO concentration. (a) 20% RH; (b) 70% RH.

Table S1. Reactions added to the MCM model and their corresponding rate constants.

No.	Reactions	Rate (cm^3 $molecule^{-1}$ s^{-1} or s^{-1})
1	$N_2O + O^1D \rightarrow NO+NO$	7.6×10^{-11}
2	$O^1D + CO_2 \rightarrow O + CO_2$	$7.5\times10^{-11}\times e^{115/T}$
3	$O^1D + H_2 \rightarrow OH + H$	1.2×10^{-10}
4	$O^1D + N_2 + M \rightarrow N_2O$	$2.8\times10^{-36}\times(300/T)^{0.88}$
5	$O + OH \rightarrow O_2 + H$	$2.4\times10^{-11}\times e^{110/T}$
6	$O + HO_2 \rightarrow O_2 + OH$	$3.0\times10^{-11}\times e^{200/T}$
7	$O + H_2O_2 \rightarrow HO_2 + OH$	$1.4\times10^{-12}\times e^{-2000/T}$
8	$O + HO_2NO_2 \rightarrow$ products	$7.8\times10^{-11}\times e^{-3400/T}$
9	$H + O_3 \rightarrow OH + O_2$	$1.4\times10^{-10}\times e^{-470/T}$
10	$H + HO_2 \rightarrow OH + OH$	7.2×10^{-11}
11	$H + HO_2 \rightarrow O + H_2O$	1.6×10^{-12}
12	$H + HO_2 \rightarrow O_2 + H_2$	6.9×10^{-12}
13	$H + NO_2 \rightarrow NO + OH$	$4.0\times10^{-10}\times e^{-340/T}$
14	$NO_3 + NO_3 \rightarrow O_2 + NO_2 + NO_2$	$8.5\times10^{-13}\times e^{-2450/T}$
15	$N_2O_5 + H_2O \rightarrow HNO_3 + HNO_3$	2.0×10^{-21}
16	$HCHO + HO_2 \rightarrow HOCH_2O_2$	$9.7\times10^{-15}\times e^{625/T}$
17	$HOCH_2O_2 \rightarrow HO_2 + HCHO$	$2.4\times10^{12}\times e^{-7000/T}$
18	$HOCH_2O_2 + HO_2 \rightarrow HOCH_2O_2H$	$5.6\times10^{-15}\times e^{2300/T}\times0.5$
19	$HOCH_2O_2 + HO_2 \rightarrow HCOOH$	$5.6\times10^{-15}\times e^{2300/T}\times0.3$
20	$HOCH_2O_2 + HO_2 \rightarrow OH + HOCH_2O$	$5.6\times10^{-15}\times e^{2300/T}\times0.2$
21	$HOCH_2O_2 + NO \rightarrow NO_2 + HOCH_2O$	5.6×10^{-12}
22	$HOCH_2O_2 + HOCH_2O_2 \rightarrow HCOOH + HOCH_2OH$	$5.7\times10^{-14}\times e^{750/T}$
23	$HOCH_2O_2 + HOCH_2O_2 \rightarrow HOCH_2O + HOCH_2O$	5.5×10^{-12}
24	$HOCH_2O_2H + OH \rightarrow HOCH_2O_2$	$3.1\times10^{-11}\times0.12$
25	$HOCH_2O_2H + OH \rightarrow HCOOH + OH$	$3.1\times10^{-11}\times0.88$
26	$HOCH_2O \rightarrow HCOOH + HO_2$	5×10^{14}
27	$HOCH_2OH + OH \rightarrow HCOOH + HO_2$	1.1×10^{-11}
28	$CH_3CHO \rightarrow VINOH$	$J_{13}\times1.5 + 1.17\times10^{-19}\times T^{1.2}\times e^{-279.8/T}\times$[Acids][a]
29	$VINOH \rightarrow CH_3CHO$	$4.67\times10^{-26}\times T^{3.3}\times e^{2269/T}\times$[Acids][a]
30	$VINOH + OH \rightarrow HCOOH + OH + HCHO$	3.8×10^{-11}
31	$VINOH+OH\rightarrow HOCH_2CHO + HO_2$	2.4×10^{-11}
32	$VINOH + OH \rightarrow VINOHOHO_2$	5.2×10^{-12}
33	$VINOHOHO_2 + NO \rightarrow HCOOH + HCHO + NO_2$	1.0×10^{-11}
34	$OH + HCHO \rightarrow HCOOH + HO_2$	2.0×10^{-13}
35	$CH_3O_2 + OH \rightarrow CH_2OOA$	2.8×10^{-10}
36	$CH_2OOA \rightarrow CH_2OO$	KDEC×0.37[b]
37	$CH_2OOA \rightarrow CO$	KDEC×0.50
38	$CH_2OOA \rightarrow HO_2 + CO + OH$	KDEC×0.13
39	$CH_2OO+CO \rightarrow HCHO$	1.2×10^{-15}
40	$CH_2OO + NO \rightarrow HCHO + NO_2$	1.0×10^{-14}
41	$CH_2OO + NO_2 \rightarrow HCHO + NO_3$	1.0×10^{-15}
42	$CH_2OO \rightarrow HCHO + H_2O_2$	$6.0\times10^{-18}\times H_2O$
43	$CH_2OO \rightarrow HCOOH$	$1.0\times10^{-18}\times H_2O$
44	$HCOOH + OH \rightarrow HO_2$	4.5×10^{-13}

[a]The model considers the combined concentrations of formic acid and acetic acid; J_{13} is the photolysis rate of acetaldehyde. [b]KDEC = 1×10^6.

Table S2. Key input parameters used in the box model simulations.

No.	Parameters	Values
1	RH	20% or 70%
2	T	298 K
3	Toluene	94 ppbv
4	Ozone	1580 ppbv
5	N_2O	(0, 0.01, 0.02, 0.04, 0.06, 0.08, and 0.1) × M[a]
6	$J_{O_3 \rightarrow O^1D}$	3.01×10^{-2} s^{-1}
7	Residence time	3.9, 15.8, 27.5, 39.3, 51.0, and 60.0 s

[a]M denotes the total gas number density.

Table S3. The derived equivalent •OH exposures under different experimental conditions.

Number of lamps illuminated	Positions of sample collection[a]	Residence time (s)	Modeled •OH concentration (molecules cm^{-3})		Equivalent •OH exposures (days)	
			20% RH	70% RH	20% RH	70% RH
1	5%	3.9	5.21×10^9	1.59×10^{10}	0.07	0.20
1	25%	15.8	3.15×10^9	8.77×10^9	0.16	0.44
1	45%	27.5	2.69×10^9	1.05×10^{10}	0.24	0.93
1	65%	39.3	2.67×10^9	1.20×10^{10}	0.34	1.52
1	85%	51.0	2.62×10^9	1.48×10^{10}	0.43	2.43
2	85%	51.0	6.04×10^9	4.33×10^{10}	0.99	7.10
4	85%	51.0	1.93×10^{10}	8.04×10^{10}	3.16	13.18
6	85%	51.0	3.16×10^{10}	9.33×10^{10}	5.19	15.30
8	85%	51.0	3.87×10^{10}	9.54×10^{10}	6.34	15.64

[a] axial length of the OFR

Table S4. The modeled concentrations of •OH, HO_2•, and NO, as well as the ratio of NO:HO_2• under different experimental conditions with the addition of N_2O.

No.	Initial N_2O (%)	•OH (molecules cm^{-3})		HO_2• (molecules cm^{-3})		NO (ppbv)		NO:HO_2•	
		20%RH	70%RH	20%RH	70%RH	20%RH	70%RH	20%RH	70%RH
0	0%	2.92×10^9	1.90×10^{10}	9.45×10^9	1.19×10^{10}	0.00	0.0	0.00	0.0
1	1%	1.97×10^9	1.37×10^{10}	1.67×10^{10}	1.72×10^{10}	1.82	0.6	2.7	0.9
2	2%	1.40×10^9	9.51×10^9	1.38×10^{10}	2.42×10^{10}	4.78	2.1	8.5	2.2
3	4%	6.88×10^8	4.59×10^9	5.05×10^9	1.90×10^{10}	11.36	6.6	55.3	8.6
4	6%	3.95×10^8	2.40×10^9	2.21×10^9	1.04×10^{10}	17.66	12.0	196.4	28.4
5	8%	2.56×10^8	1.41×10^9	1.18×10^9	5.71×10^9	23.4	17.5	489.4	75.3
6	10%	1.80×10^8	9.18×10^8	7.09×10^8	3.42×10^9	28.7	22.7	995.1	163.1

References

Peng, Z., Palm, B. B., Day, D. A., Talukdar, R. K., Hu, W., Lambe, A. T., Brune, W. H., and Jimenez, J. L.: Model Evaluation of New Techniques for Maintaining High-NO Conditions in Oxidation Flow Reactors for the Study of OH-Initiated Atmospheric Chemistry, ACS Earth Space Chem., 2, 72–86, https://doi.org/10.1021/acsearthspacechem.7b00070, 2018.